

Real-Time X-Ray Studies of Strain Kinetics in $\text{In}_x\text{Ga}_{1-x}\text{As}$ Quantum Well Structures

R. Clarke and W. Dos Passos

Department of Physics, University of Michigan, Ann Arbor, Michigan 48109

W. Lowe

AT&T Bell Laboratories, Murray Hill, New Jersey 07974

B. G. Rodricks and C. Brizard

Advanced Photon Source Division, Argonne National Laboratory, Argonne, Illinois 60439

(Received 13 August 1990)

A new time-resolved x-ray method of probing the kinetics of interfacial strains in semiconductor heterostructures is presented. High-resolution synchrotron-radiation measurements of the strain relaxation during rapid thermal annealing show that the lattice dilation of an as-grown quantum well structure is relieved cooperatively by a series of sluggish discontinuous transitions. Well-defined metastable states of strain are observed between the transitions.

PACS numbers: 61.10.Lx, 68.35.Rh, 81.40.Ef

Interfacial mismatch is often used to build elastic strain into epitaxial materials, resulting in modifications of the band structure, electronic transport, and optical properties.¹ The strains encountered can be quite substantial and would require many GPa of externally applied pressure to achieve the same level of lattice distortion by mechanical means. One of the most interesting aspects of strained-layer epitaxy is that the physics is controlled largely by structural kinetics.^{2,3} For example, activation barriers to dislocation motion and migration in covalently bonded semiconductors are known to promote coherently strained layers which are far thicker than would be predicted from purely thermodynamic considerations.⁴

While there has been a great deal of work, both theoretical and experimental, devoted to strained layers in heteroepitaxial materials very little is known as yet about the microscopic kinetic processes involved. How are large coherent elastic strains established and sustained in such materials and what are the kinetic aspects of the mechanisms responsible for strain relaxation? These issues are part of the larger picture of nonequilibrium systems whose dynamical behavior is predicated by the existence of many metastable states with similar free energies. The approach to "equilibrium" in such systems by means of various annealing processes is an interesting yet still unsolved problem of current interest in statistical mechanics.⁵ From a practical standpoint an understanding of annealing is important across the whole spectrum of materials from polymers to superconductors.

In this Letter we present results on a real-time study of the interface structure of a strained-layer quantum well during rapid thermal annealing. The system we have chosen for these experiments is a single quantum well (SQW) fabricated from III-V compound semiconductors. The SQW structure is particularly advanta-

geous here because the interference of x rays from the different layers permits high-precision measurement of the magnitude and profile of the layer-to-layer epitaxial strain. The measurements, obtained in a time-resolved mode by specially developed synchrotron-radiation techniques, reveal an unexpectedly complex pathway of interfacial strain kinetics by means of which the entire SQW structure attains its ideal, stable, state. In particular, we show that interfacial strain relaxation is not, as previously believed, a gradual process occurring through local misfit dislocation migration but a discontinuous, *cooperative* mechanism which proceeds via a sequence of partially ordered metastable states.

The samples studied in these experiments consist of a thin (~ 180 Å) layer of $\text{In}_x\text{Ga}_{1-x}\text{As}$ ($x \approx 0.05$) sandwiched between relatively thick (2000–3000 Å) GaAs layers to form a single quantum well. The structures (Fig. 1) are grown by molecular-beam epitaxy on semi-insulating GaAs(100) substrates held⁶ at $T = 520^\circ\text{C}$ in order to minimize In segregation.⁷ However, the sluggish kinetics at this temperature inhibits the development of coherent long-range crystalline order within the layers. Interrupted growth (waiting for a few minutes after the growth of each layer) is sometimes used to overcome

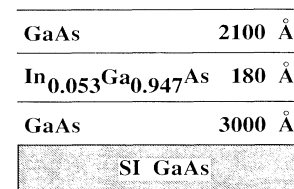


FIG. 1. Schematic of $\text{In}_x\text{Ga}_{1-x}\text{As}$ single quantum well structure.

this problem.⁶ Alternately, as will be shown below, the structure can be brought to a pseudomorphic coherent state by post-growth annealing.⁸

The new time-resolved x-ray technique employed in these studies is based on curved-crystal optics originally developed by Lemonnier *et al.*⁹ A "white" beam of synchrotron radiation is incident on an asymmetrically cut Ge(111) monochromator crystal. The outgoing beam has an energy bandwidth given by¹⁰

$$\frac{\Delta E}{E} = \cot\theta[\omega_{\text{acc}}^2 + (a_1 + a_2 + a_3)^2]^{1/2}, \quad (1)$$

where θ is the Bragg angle corresponding to energy E , ω_{acc} is the acceptance of the curved crystal, and

$$a_1 = \frac{h}{p}, \quad a_2 = \frac{1}{2} \left| \frac{\sin(\theta + \alpha)}{p} - \frac{\sin(\theta - \alpha)}{p'} \right|,$$

$$a_3 = l \sin(\theta + \alpha) \left| \frac{1}{2p} - \frac{1}{2p - w} \right|.$$

Here, w is the length of the source, h is the horizontal source size, l is the illuminated length of the Ge crystal, and α is the asymmetric cut angle. p and p' are the source-to-monochromator and monochromator-to-focus distances, respectively. A plot of Eq. (1) is shown in Fig. 2. Our measurements are performed at a focus condition such that $\Delta E/E$ is a minimum, giving the optimum resolution ($\sim 10^{-4}$). In this condition the curved crystal gives an essentially monochromatic x-ray beam which is angularly dispersed over a range of 250 arcsec. The angular dispersion, in conjunction with a position-sensitive detector, permits each point of a rocking curve to be recorded simultaneously. Using this dispersive technique

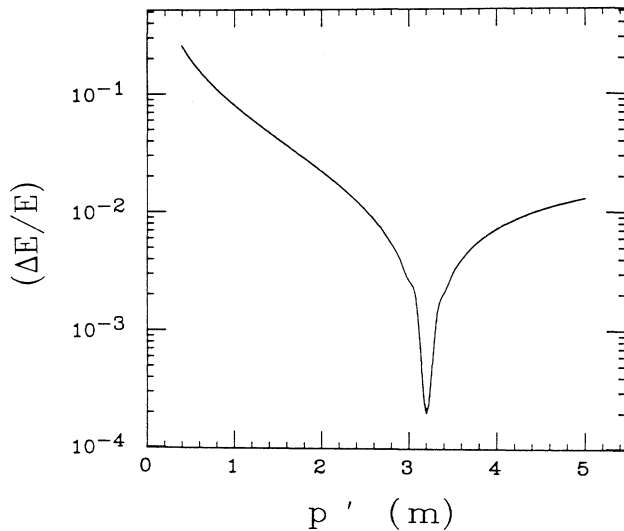


FIG. 2. Calculated energy dispersion of synchrotron beam from the asymmetric-cut Ge(111) curved crystal as a function of focal distance p' .

complete rocking curves from the SQW can be recorded in rapid succession.

At the heart of our time-resolved measurements is a radiation-hardened charge-coupled-device (CCD) detector consisting of 340×580 pixels each $22.5 \mu\text{m}$ square. The operation and characteristics of the detector have been described previously.¹¹ In order to collect real-time data, a horizontal slit is used to mask the surface of the CCD chip. The slit opening is adjusted to expose three rows ($75 \mu\text{m}$) of the CCD to the diffracted beam. After a predetermined exposure time (~ 100 msec in this experiment) the charge collected on the exposed area is transferred to the masked area of the chip using the parallel row-transfer register. In this mode the detector operates as a "streak camera" recording one-dimensional diffraction information with a time resolution determined by the speed of the parallel transfer ($\sim 20 \mu\text{sec/row}$ in the present detector). The CCD is oriented such that the horizontal angular dispersion of the beam is utilized to record a moderately high-resolution ($\Delta\omega = 10$ arcsec) diffraction profile of the SQW sample; each pixel receives a signal corresponding to the reflectivity at a particular rocking angle.

Figure 3 compares the rocking curves of an SQW sample prepared without growth interruption. The sample is examined by conventional double-crystal diffraction in nondispersive (+ -) geometry, before and after rapid thermal annealing. It is clear that marked irreversible changes take place. For example, before annealing [Fig. 3(a)] the rocking profile is asymmetric and shows two small interference fringes to the low-angle side of the substrate peak. Modeling of the interface structure using dynamical scattering theory¹² reveals that these

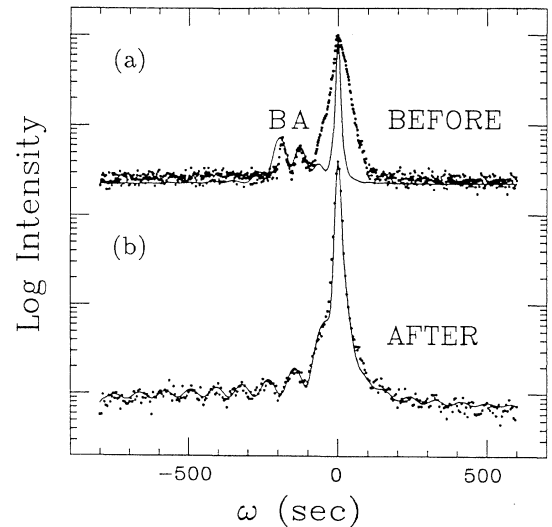


FIG. 3. (400) rocking curves of SQW: (a) as-grown; (b) after rapid thermal annealing. The solid lines are fits by a dynamical scattering model (Ref. 12).

fringes arise because part of the GaAs buffer layer (the upper ~ 1000 Å) and the whole of the GaAs capping layer (2100 Å) are slightly dilated, in the direction perpendicular to the layers, by $\epsilon_{\perp} = 5.3 \times 10^{-4}$ with respect to bulk GaAs. The origin of this distortion, which has been observed in other cap-layer configurations,¹³ is not clear, although the presence of a significant as-grown density of twins and dislocations [$\sim 5 \times 10^9$ cm⁻², as estimated from the broadening of the $\omega = 0$ peak in Fig. 3(a)] could well be responsible. After annealing [Fig. 3(b)] the rocking curve exactly matches the calculated curve for an *ideal coherent structure* with pseudomorphic In_xGa_{1-x}As and completely relaxed GaAs buffer and cap layers. Note also the dramatic sharpening of the $\omega = 0$ peak after annealing and the appearance of the *Pendellösung* fringes which arise from a phase shift of the waves scattered from the substrate (buffer) relative to those coherently scattered from the GaAs cap layer. The positions of the *Pendellösung* fringes are a sensitive measure of the thickness of the InGaAs layer and its strain.¹⁴ It is interesting to note that we obtain identical data [Fig. 3(b)] without annealing if growth interruption is employed.

Now we turn to the time-resolved data. Figure 4 shows the variation in position of the peaks in the rocking curve, measured now by the real-time dispersive

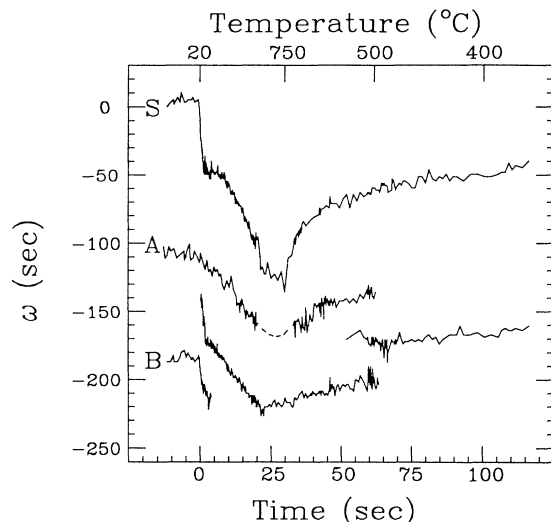


FIG. 4. X-ray peak position at CCD detector as a function of time during rapid thermal annealing. A quartz-halogen heating lamp is turned on at $t=0$ and off at $t=30$ sec during which the sample temperature reaches 750°C (as measured by thermocouples in front of, and behind, the sample). Curves *A* and *B* refer to the peaks in Fig. 3(a) and their positions are measured with reference to the initial position ($\omega=0$) of the substrate peak. Curve *S* corresponds to scattering from the substrate and unstrained GaAs layers. The dashed portion of curve *A* is where it merges with the very intense substrate peak.

technique, as the SQW is undergoing rapid thermal annealing (RTA). The time-resolved data, when analyzed each 100 msec using the same interference model as for the static results in Fig. 3, show the dynamic evolution of the SQW from the as-grown inhomogeneous strain configuration to the ideal relaxed state.

In addition to the substrate-peak shifts (upper curve) caused by thermal expansion and contraction, there are many interesting and previously unobserved transitions during the RTA run shown in Fig. 4. We focus our attention first on the behavior of the two interference fringes (*A, B*) in the as-grown sample. On heating, the outer fringe (*B*) shifts to lower angle and soon after undergoes a sudden shift in the opposite direction. The shift to lower angles is caused by the differential thermal expansion between the InGaAs layer and the GaAs layers and the upward shift occurs as the resulting mismatch strains at the interfaces are suddenly relieved. On cooling, a reverse differential thermal-expansion process is observed and subsequently (at $t=50$ sec) a strongly discontinuous transition takes place where *A* and *B* are replaced by a single peak. The dynamical scattering analysis of this phase reveals that the dilation of the GaAs at the InGaAs-buffer-layer interface has relaxed at this transition but the cap layer is still strained. At later times, not shown in Fig. 4, there is a further discontinuous transition (at $\sim 300^\circ\text{C}$) involving the remaining interference peak ($\omega \approx -170$ arcsec) where the lattice spacing of the GaAs cap layer relaxes to its bulk value.

In this way the inhomogeneous strain relaxation of the thick GaAs layers of the SQW starts at the substrate, as one would expect, and proceeds upwards to the GaAs cap of the In_xGa_{1-x}As layer. The important point is that the strain relaxes discontinuously and cooperatively in each of the GaAs segments of the SQW. Interestingly, it appears that macroscopic strained and unstrained GaAs regions of the sample can coexist in the same layer for relatively long intervals (~ 10 sec in the example presented here). This behavior is consistent with very sluggish kinetics of dislocation motion at temperatures below 500°C . A mean velocity of dislocation migration of $\lesssim 0.1 \mu\text{msec}^{-1}$ can be inferred from the temporal coexistence limits in Fig. 4. This is, however, much faster than the glide velocities ($< 0.01 \mu\text{msec}^{-1}$) measured¹⁵ by electron microscopy in Si/Ge_xSi_{1-x}/Si SQW's and is consistent with the lower Peierls barriers in the III-V systems.

In conclusion, our new method of probing interface strains in a time-resolved mode has shed new light on the global kinetics of strained-layer structures. The results emphasize the cooperative nature of the relaxation mechanism, involving transitions between partially ordered metastable states of strain. The existence of well-defined, albeit metastable, states of strain in complex multilayered heterostructures may be of practical in-

terest in establishing reliable thermal-processing procedures for such systems.

This work was supported in part by NSF Grant No. DMR8805165 and by the ARO Universities Research Initiative program under Grant No. DAAL-03-87-K0007. We are grateful to Yi-Jen Chan for providing MBE samples and to R. Hull and D. Pavlidis for useful discussions. The synchrotron studies were done at the National Synchrotron Light Source on the X-16B beam line. The NSLS is supported by the U.S. DOE, Basic Energy Sciences Materials and Chemical Sciences under Contract No. DE-AC02-76CA0016.

¹See *Layered Structures, Epitaxy and Interfaces*, edited by J. M. Gibson and L. R. Dawson, MRS Symposia Proceedings No. 37 (Materials Research Society, Pittsburgh, 1985).

²R. Bruinsma and A. Zangwill, *J. Phys. (Paris)* **47**, 2055 (1986).

³J. Y. Tsao, B. W. Dodson, S. T. Picraux, and D. M. Cornelson, *Phys. Rev. Lett.* **59**, 2455 (1987).

⁴I. J. Fritz, P. L. Gourley, and L. R. Dawson, *Appl. Phys. Lett.* **51**, 1004 (1987).

⁵See, for example, *Heidelberg Colloquium on Glassy Dynamics*, edited by J. L. van Hemmen and I. Morgenstern, Lecture Notes in Physics Vol. 275 (Springer-Verlag, New York, 1987).

⁶P. R. Berger, P. K. Bhattacharya, and J. Singh, *J. Appl. Phys.* **61**, 2856 (1987).

⁷J. T. Ebner and J. R. Arthur, *J. Vac. Sci. Technol. A* **5**, 2007 (1987).

⁸Note that the strained layer is well below the critical thickness for misfit dislocation formation. P. J. Orders and B. F. Usher, *Appl. Phys. Lett.* **50**, 980 (1987).

⁹M. Lemonnier, R. Fourme, F. Rousseaux, and R. Kahn, *Nucl. Instrum. Methods* **152**, 173 (1978).

¹⁰W. Schildkamp, *Nucl. Instrum. Methods Phys. Res., Sect. A* **266**, 479 (1988).

¹¹B. Rodricks, R. Clarke, R. Smither, and A. Fontaine, *Rev. Sci. Instrum.* **60**, 2586 (1989).

¹²The diffraction profiles are calculated in the two-beam approximation with a modified version of the code developed by B. K. Tanner and M. J. Hill, *Adv. X-Ray Anal.* **29**, 337 (1986).

¹³M. Gal, P. J. Orders, B. F. Usher, M. J. Joyce, and J. Tann, *Appl. Phys. Lett.* **53**, 113 (1988).

¹⁴L. Tapfer and K. Ploog, *Phys. Rev. B* **40**, 9802 (1989).

¹⁵R. Hull and J. C. Bean, *Appl. Phys. Lett.* **55**, 1900 (1989).